Quantum entanglement between signal and frequency-up-converted idler photons

Jiaxuan Wang [1,2] Alexei V. Sokolov [1,2] and Girish S. Agarwal [1,2,3]
[1] *Department of Physics and Astronomy, Texas A&M University, College Station, Texas 77843, USA*
[2] *Institute for Quantum Science and Engineering, Texas A&M University, College Station, Texas 77843, USA*
[3] *Department of Biological and Agricultural Engineering, Texas A&M University, College Station, Texas 77843, USA*

(Received 8 May 2023; accepted 17 November 2023; published 8 December 2023)

Quantum frequency up-conversion is a cutting-edge technique that leverages the interaction between photons and quantum systems to shift the frequency of single photons from a lower frequency to a higher frequency. If a photon before up-conversion was part of an entangled pair, it becomes crucial to comprehend the time-frequency entanglement after up-conversion. In this study, we present a theoretical analysis of the transformation of the time-dependent second-order quantum correlations in photon pairs and find the preservation of such correlations under fairly general conditions. Furthermore, we analyze Hong-Ou-Mandel interference between the signal and frequency-converted idler photons to gain insight into the indistinguishability of the two photons. The visibility of two-photon interference is sensitive to the magnitude of frequency conversion and improves as the frequency separation between two photons decreases.

DOI: 10.1103/PhysRevA.108.063706

I. INTRODUCTION

Optical frequency up-conversion has been the subject of much interest and investigation since its discovery in 1967 by Midwinter and Warner [1]. The driving factor behind the importance of up-conversion [2] has been the possibility of detecting infrared radiation [3–7] by converting it to the optical domain as the detection technology in the optical domain is much better. This is because photons of visible light carry more energy and can be detected using the well-developed Si-based detector technology. Thus, techniques for improving the efficiency of the up-conversion process have been developed [8,9]. The improved efficiency is important for many applications, for example, in imaging [10,11]. Of particular importance in the context of quantum technologies is the up-conversion of a single photon. The quantum theory of the up-conversion process has been developed [12,13]. With the growing interest in quantum entanglement, Kumar *et al.* [8,14,15] demonstrated preservation of the quantum correlations between up-converted idler photons and signal photons produced by an optical parametric amplifier. In particular, they showed the survival of the nonclassical intensity correlation between two photons at 1064 nm when one of these was converted to 532 nm. Since these early experiments, the interest shifted to single photons, and several experiments studied the quality of the up-converted single photons [16,17] and verified the preservation of quantum correlations during the process [18–20]. As known, a versatile source of single photons is the spontaneous parametric down-conversion process where one has entangled pairs, i.e., signal and idler photons whose frequencies can be quite different, still exhibiting strong second-order quantum correlations represented by $g^{(2)}(\tau)$. Direct measurement of $g^{(2)}(\tau)$ is difficult as the correlation time could be 100 fs or less, and one uses the second-order Hong-Ou-Mandel (HOM) interference [21–28] for getting information at these timescales. In a recent work [29,30] the correlation time was about 80 ps [31] and the frequency of the idler photon was up-converted by about 120 THz. Tyumenev *et al.* [29] demonstrated the preservation of such correlation time between the signal and up-converted idler photons.

The main purpose of our paper is twofold. First, we provide a theoretical framework to the observation of Tyumenev *et al.* [29] on the preservation of time correlation. Second, we examine the degree of indistinguishability between the two photons of the pair before and after up-conversion. The organization of the paper is as follows. In Sec. II, we present a first-principle theoretical calculation of the nonclassical time correlations between the signal photon and the up-converted or down-converted idler photon. We find the preservation of such correlations under fairly general conditions. This theoretical result is consistent with the observations reported in [29]. In Sec. III, we analyze the two-photon HOM interference between the signal and frequency-converted idler photons. The visibility of the two-photon interference is sensitive to the magnitude of the frequency conversion, and it improves when the frequency separation between two photons decreases. Our theoretical results on HOM interference are relevant to several experiments, for example, Refs. [18–20] on the quality of frequency-converted single photons. Our results also apply to cases when the frequency is down-converted, though we primarily focus on up-conversion processes. We present in Sec. IV concluding remarks.

II. SECOND-ORDER CORRELATION OF SIGNAL AND FREQUENCY UP-CONVERTED IDLER PHOTONS

As illustrated in Fig. 1, we study the entangled state [32], which consists of a signal photon with frequency ω_s and an idler photon with frequency ω_i,

$$|\Phi\rangle = \iint d\omega_s d\omega_i f(\omega_s, \omega_i) a_s^{\dagger}(\omega_s) a_i^{\dagger}(\omega_i) |0, 0\rangle, \qquad (1)$$

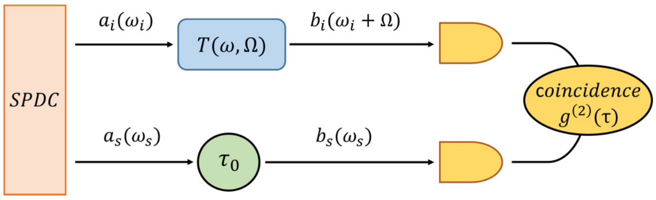

FIG. 1. Experimental setup for the detection of second-order correlation $g^{(2)}(\tau)$ of the signal and frequency-converted idler photons, where a positive (negative) Ω value stands for up (down)-conversion.

where $a^\dagger_{s(i)}(\omega_{s(i)})$ is the creation operator for the signal (idler) mode, which satisfies the commutation relation $[a_{s(i)}(\omega), a^\dagger_{s(i)}(\omega')] = \delta(\omega-\omega')$, and $[a_{s(i)}(\omega), a_{i(s)}(\omega')]$ $= [a_{s(i)}(\omega), a^\dagger_{i(s)}(\omega')] = 0$. The entanglement between signal and idler photons arises from the nonfactorization of the two-mode frequency distribution $f(\omega_s,\omega_i)$. We consider the input photon frequency distribution following an entangled Gaussian distribution [33]

$$f(\omega_s,\omega_i) = \frac{1}{\sqrt{2\pi\sigma_p\sigma_-}} e^{-(\omega_s+\omega_i-\omega_p)^2/(16\sigma_p^2)} e^{-(\omega_i-\omega_s+\triangle)^2/(4\sigma_-^2)}, \tag{2}$$

where ω_p represents the pump frequency and σ_p is its bandwidth. $\triangle$ denotes the frequency difference between the central frequencies of ω_i and ω_s, while σ_- represents the bandwidth of the photon pairs. It is important to note that the distribution is normalized, meaning that $\iint |f(\omega_s,\omega_i)|^2 d\omega_s d\omega_i = 1$. Furthermore, it is worth mentioning that the phase-matching condition gives rise to the frequency distribution. While this distribution is inherently a sinc function, it can often be approximated by a Gaussian distribution for practical purposes. Consider next the frequency up-conversion of the idler photon. Let us assume that an idler photon of frequency $(\omega-\Omega)$ is up-converted to a photon of frequency ω. The up-conversion would involve a strong classical field of frequency Ω. Let $b_i(\omega)$ and $a_i(\omega-\Omega)$ be the annihilation operators associated with the up-converted idler photon of frequency ω and the idler photon of frequency $(\omega-\Omega)$. There are no input photons at the up-converted frequency ω. Using the well-known results from the quantum theory of frequency conversion [13,14], we write the annihilation operator for the up-converted field in terms of the annihilation operators for the fields at frequency $(\omega-\Omega)$ and ω, i.e.,

$$b_i(\omega) = T(\omega,\Omega)a_i(\omega-\Omega) + \eta(\omega,\Omega)a_v(\omega). \tag{3}$$

Here $|T(\omega,\Omega)|^2$ is the up-conversion rate and $\eta(\omega,\Omega) = \sqrt{1-|T(\omega,\Omega)|^2}$. The operator $a_v(\omega)$ represents the up-converted field at the input of the up-converter. Since there is no up-converted field at the input of the frequency-converting medium, the input state of the fields to the frequency converter is $|1_{\omega-\Omega}\rangle_i|0_\omega\rangle_v$, i.e., one photon in the idler at $(\omega-\Omega)$ and zero photon in the up-converted idler field at ω. The term $a_v(\omega)$ does not contribute to normally ordered correlations because of the initial state $|0_\omega\rangle_v$. The situation would be different if the up-converted field is present at the input to frequency converter. It is also to be noted that, though $a_v(\omega)$ does not contribute to the normally ordered correlations, it is required for the preservation of Bosonic commutation relation $[b_i(\omega), b_i^\dagger(\omega')] = \delta(\omega-\omega')$. Several experiments on frequency conversion employ modulation at the frequency Ω. Consequently, the input photons at ω undergo conversion to frequencies $\omega+\Omega$ and $\omega-\Omega$. In this context, we accommodate the frequency shift Ω in Eq. (3) to encompass both positive and negative values, allowing for both up- and down-conversion. It is worth noting that, as mentioned in the Introduction, some experiments utilized modulation in the GHz domain. Throughout this process, the frequency of the signal photon remains unchanged. In this particular setup, one photon traverses through the medium, while the other photon traverses through a vacuum. This discrepancy in their paths introduces a time delay between the two photons. Here, we introduce such a delay to the signal photon

$$b_s(\omega) = a_s(\omega)e^{-i\omega\tau_0}. \tag{4}$$

The second-order correlation $g^{(2)}(t,t+\tau)$ is defined as

$$g^{(2)}(t,t+\tau) = \langle b_i^\dagger(t)b_s^\dagger(t+\tau)b_s(t+\tau)b_i(t)\rangle. \tag{5}$$

Considering Eqs. (1), (3), and (4), and changing the modes to the frequency domain $b_i(t) = \frac{1}{\sqrt{2\pi}}\int d\omega_1 b_i(\omega_1)e^{-i\omega_1 t}$ and $b_s(t+\tau) = \frac{1}{\sqrt{2\pi}}\int d\omega_2 b_s(\omega_2)e^{-i\omega_2(t+\tau)}$, we obtain

$$\begin{aligned} b_s(t+\tau)b_i(t)\,|\Phi\rangle = \frac{1}{2\pi}\iint d\omega_1 d\omega_2 T(\omega_1,\Omega)a_s(\omega_2) \\ \times\, a_i(\omega_1-\Omega)e^{i\omega_1 t}e^{i\omega_2(t+\tau-\tau_0)}\iint d\omega_s \\ \times\, d\omega_i f(\omega_s,\omega_i)a_s^\dagger(\omega_s)a_i^\dagger(\omega_i)\,|0,0\rangle\,, \end{aligned} \tag{6}$$

which gives the result for Eq. (5) as

$$\begin{aligned} g^{(2)}(t,t+\tau) = \frac{1}{4\pi^2}\Big|\iint d\omega_1 d\omega_2 T(\omega_1,\Omega) \\ \times e^{i\omega_1 t}e^{i\omega_2(t+\tau-\tau_0)} f(\omega_1-\Omega,\omega_2)\Big|^2. \end{aligned} \tag{7}$$

Note that the term $a_v(\omega)$ in Eq. (3) has no impact on the normal-ordered correlation $g^{(2)}$. Assuming that the conversion rate remains nearly constant, denoted as $T(\omega,\Omega) = T$ within the relevant range, and implementing the parameter transformation $\Omega_1 = \omega_1 - \Omega$, we can simplify Eq. (7) to

$$\begin{aligned} g^{(2)}(t,t+\tau) = \frac{T^2}{4\pi^2}\Big|\iint d\Omega_1 d\omega_2 e^{i\Omega_1 t}e^{i\omega_2(t+\tau-\tau_0)} \\ \times\, f(\Omega_1,\omega_2)\Big|^2. \end{aligned} \tag{8}$$

Considering a photon pair following the Gaussian distribution in Eq. (2), we obtain

$$\begin{aligned} g^{(2)}(t,t+\tau) = \frac{T^2}{(2\pi)^3\sigma_p\sigma_-}\Big|\iint d\Omega_1 d\omega_2 \\ \times\, e^{i\frac{1}{2}(\omega_2+\Omega_1)[(t+\tau'-\tau_0)+t]}e^{i\frac{1}{2}(\omega_2-\Omega_1)[(t+\tau-\tau_0)-t]} \\ \times\, e^{-(\omega_2+\Omega_1-\omega_p)^2/16\sigma_p^2}e^{-(\omega_2-\Omega_1-\triangle)^2/4\sigma_-^2}\Big|^2. \end{aligned} \tag{9}$$

Through orthogonal parameter transformation to $u = (\omega_2 + \Omega_1)/\sqrt{2}$ and $v = (\omega_2 - \Omega_1)/\sqrt{2}$, the double integral simplifies into the product of two separate single-parameter integrals

$$g^{(2)}(t, t+\tau) = \frac{T^2}{(2\pi)^3\sigma_p\sigma_-}\left|\int du e^{iu(2t+\tau-\tau_0)/\sqrt{2}}\right.$$
$$\times\ e^{-(u-\omega_p/\sqrt{2})^2/(8\sigma_p^2)}\int dv e^{iv(\tau-\tau_0)/\sqrt{2}}$$
$$\left.\times\ e^{-(v-\triangle/\sqrt{2})^2/(2\sigma_-^2)}\right|^2. \tag{10}$$

It is worth mentioning that the two integrals in the expression correspond to the Fourier transforms of Gaussian functions. Thus, the shifts ω_p and $\triangle$ do not have any impact on the mode square. Consequently, we arrive at the following result:

$$g^{(2)}(t, t+\tau) = \frac{2\sigma_p\sigma_- T^2}{\pi}e^{-2\sigma_p^2(2t+\tau-\tau_0)^2}e^{-\frac{1}{2}\sigma_-^2(\tau-\tau_0)^2}. \tag{11}$$

The two-time correlation presented in Eq. (11) should be averaged over the detector's resolution time, denoted as T_R,

$$g^{(2)}(\tau) = \int_{-T_R/2}^{+T_R/2} dt g^{(2)}(t, t+\tau), \tag{12}$$

which gives

$$g^{(2)}(\tau) = \frac{1}{2\sqrt{2\pi}}\sigma_- T^2 e^{-\frac{1}{2}\sigma_-^2(\tau-\tau_0)^2}[\mathrm{erf}(\sqrt{2}\sigma_p(\tau-\tau_0+T_R))$$
$$-\ \mathrm{erf}(\sqrt{2}\sigma_p(\tau-\tau_0-T_R))], \tag{13}$$

where $\mathrm{erf}(x)$ stands for the error function. Note that, when there is no conversion, $T = 1$, $\tau_0 = 0$, and Eq. (13) will be the correlation of the photons produced by the down-converter. Thus, the functional form of the time correlation is essentially preserved. This includes dependence on the detector's resolution time.

In this analysis, we examine two scenarios. In the first scenario, we assume that the large-detection time condition is met, specifically, when $\sigma_p T_R \rightarrow \infty$ and $T_R \gg \tau - \tau_0$. This condition is satisfied, for instance, when T_R is on the order of 10 : ps or 100 : ps. Under these circumstances, we derive

$$g^{(2)}(\tau) = \frac{\sigma_- T^2}{\sqrt{2\pi}}e^{-\frac{1}{2}\sigma_-^2(\tau-\tau_0)^2}. \tag{14}$$

The height of the peak is proportional to T^2, representing the probability of frequency conversion. The full width at half maximum (FWHM) of $g^{(2)}(\tau)$ between the signal and up-converted idler photons remains identical to that between the original photon pairs. This is illustrated in Fig. 2, where $g^{(2)}(\tau)$ (by dropping the factor T^2) is plotted for the signal and up-converted idler photons, revealing only a peak shift

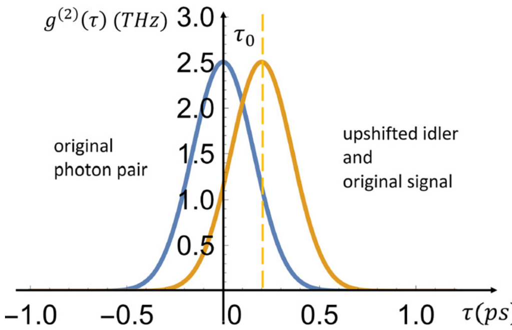

FIG. 2. The second-order correlation $g^{(2)}(\tau)$ in Eq. (13) of the signal and frequency up-converted idler photons (yellow), compared to $g^{(2)}(\tau)$ of the original photon pair (blue), for $\sigma_- = 2\pi \times 1\ THz$, $\sigma_p = \sigma_-/10$, $\tau_0 = 0.2\ ps$ and $T_R = 100\ ps$.

attributable to the difference in path length. It is worth noting that Fig. 2 is generated using the precise result outlined in Eq. (13).

In the second scenario, as $\sigma_p T_R \rightarrow 0$ and $\sigma_p(\tau - \tau_0) \rightarrow 0$, but T_R and τ can be of comparable magnitude, we derive the following expression:

$$g^{(2)}(\tau) = \frac{2T_R\sigma_p\sigma_- T^2}{\pi}e^{-\frac{1}{2}\sigma_-^2(\tau-\tau_0)^2}. \tag{15}$$

In both of these limiting cases, the $g^{(2)}(\tau)$ function is exactly the same as the correlation observed in the absence of up-conversion, with the only difference being a multiplication by T^2 and a phase shift of τ_0. This aligns with the findings of the experiment detailed in Ref. [29], where the pertinent parameters encompass $\sigma_- = 1/80$: ps, $T_R = 50$: ps, and σ_p approximately equals $2\pi \times 1$: GHz. In this context, the time correlation $g^{(2)}(\tau)$ experiences a shift due to the delay introduced by the up-conversion medium. Furthermore, the magnitude of $g^{(2)}(\tau)$ is directly proportional to T^2, a value that is diminished compared to that of $g_0^{(2)}(\tau)$.

Now, we delve into the impact of phase-matching on the two-photon correlation during the up-conversion process. To investigate this, we introduce a modification to the factor $T(\omega, \Omega)$, which is expressed as

$$T(\omega, \Omega) = Te^{-(\omega-\omega_{i0})^2/(2\beta^2)}. \tag{16}$$

In this expression, the conversion rate achieves its maximum at ω_{i0} to optimize the conversion process and decreases significantly beyond the range indicated by β. We proceed to update Eqs. (11) and (13) as follows:

$$g^{(2)}(t, t+\tau) = \frac{4T^2\beta^2\sigma_p\sigma_-}{\pi\left(2\beta^2 + 4\sigma_p^2 + \sigma_-^2\right)}$$
$$\times \exp\left[-\frac{\Omega^2 + 16\sigma_p^2\sigma_-^2(t+\tau-\tau_0)^2}{2\left(2\beta^2 + 4\sigma_p^2 + \sigma_-^2\right)}\right.$$
$$\left.-\ \frac{+4\beta^2\sigma_p^2(2t+\tau-\tau_0)^2 + \beta^2\sigma_-^2(\tau-\tau_0)^2}{\beta^2 + 4\sigma_p^2 + \sigma_-^2}\right], \tag{17}$$

and

$$g^{(2)}(\tau)=\frac{T^2\beta^2\sigma_-}{\sqrt{2\pi\left(2\beta^2+4\sigma_p^2+\sigma_-^2\right)(\sigma_-^2+2\beta^2)}}\exp\left[-\frac{\Omega^2}{2\left(2\beta^2+4\sigma_p^2+\sigma_-^2\right)}-\frac{\beta^2\sigma_-^2(\tau-\tau_0)^2}{\left(2\beta^2+4\sigma_p^2+\sigma_-^2\right)}\right]$$
$$\times\exp\left[-\frac{4(\tau-\tau_0)^2\beta^2\sigma_-^2\sigma_p^2}{(2\beta^2+4\sigma_p^2+\sigma_-^2)(\sigma_-^2+2\beta^2)}\right]\left\{\mathrm{erf}\left[\sqrt{\frac{2(\sigma_-^2+2\beta^2)}{2\beta^2+4\sigma_p^2+\sigma_-^2}}(2\tau-2\tau_0+T_R)\right]\right.$$
$$\left.-\,\mathrm{erf}\left[\sqrt{\frac{2(\sigma_-^2+2\beta^2)}{2\beta^2+4\sigma_p^2+\sigma_-^2}}(2\tau-2\tau_0-T_R)\right]\right\}. \tag{18}$$

The expressions in Eqs. (17) and (18) reduce to Eqs. (11) and (13) when $\beta^2\to\infty$. Under the condition where $T_R\gg(\tau-\tau_0)$, we observe that

$$g^{(2)}(\tau)\propto\exp\left[-\frac{\Omega^2}{2\left(2\beta^2+4\sigma_p^2+\sigma_-^2\right)}-\frac{\beta^2\sigma_-^2}{(\sigma_-^2+2\beta^2)}\times(\tau-\tau_0)^2\right], \tag{19}$$

showing explicit dependence on the parameter β and the frequency change Ω.

III. HONG-OU-MANDEL MEASUREMENT OF THE SIGNAL AND FREQUENCY-CONVERTED IDLER PHOTONS

The HOM interferometer [21,34,35] serves as a widely employed tool for measuring the biphoton joint frequency distribution, particularly effective on timescales of around tens of femtoseconds, as illustrated in Refs. [33,36–38]. Consequently, we embark on an exploration of two-photon interference involving the signal and up-converted idler photons. To facilitate this study, we introduce a tunable delay denoted as τ_T in the signal photon's path, as depicted in Fig. 3. This setup enables us to examine the impact of both the frequency shift Ω and the delay on coincidence detection on coincidence detection. For the signal photon,

$$b_s(\omega)=a_s(\omega)e^{-i\omega(\tau_T+\tau_0)}, \tag{20}$$

while the idler photon travels through the same up-conversion medium. Following the frequency conversion process, the two photons are then reunited at a 50:50 beam-splitter. The output

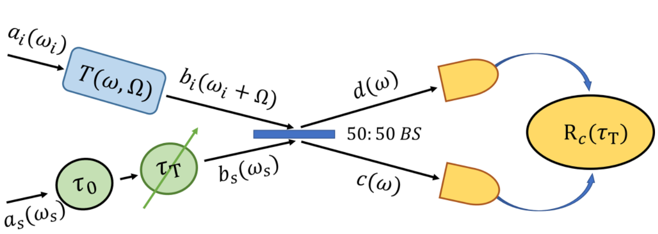

FIG. 3. Experimental setup for the HOM measurement of the signal and frequency-converted idler photons, where τ_T is a tunable delay. A positive (negative) Ω value stands for up (down)-conversion.

from this beam-splitter is represented as

$$c(\omega)=\frac{b_i(\omega)+ib_s(\omega)}{\sqrt{2}},$$
$$d(\omega)=\frac{ib_i(\omega)+b_s(\omega)}{\sqrt{2}}. \tag{21}$$

As a result, the averaged coincidence rate of the output fields

$$R_c(\tau_T)=\int dt\int d\tau\langle d^\dagger(t)c^\dagger(t+\tau)c(t+\tau)d(t)\rangle \tag{22}$$

is measured, where we assume the detection time is much larger than the pump correlation time $1/\sigma_p$ and the entanglement time $1/\sigma_-$. Changing the modes to the frequency domain $d(t)=\frac{1}{\sqrt{2\pi}}\int d\omega_1 d(\omega_1)e^{-i\omega_1 t}$ and $c(t+\tau)=\frac{1}{\sqrt{2\pi}}\int d\omega_2 c(\omega_2)e^{-i\omega_2(t+\tau)}$, we obtain

$$R_c(\tau_T)=\frac{1}{2}\left[\iint d\omega_1 d\omega_2 f^*(\omega_1-\Omega,\omega_2)f(\omega_1-\Omega,\omega_2)\times T^*(\omega_1,\Omega)T(\omega_1,\Omega)-\iint d\omega_1 d\omega_2 f^*(\omega_1-\Omega,\omega_2)f(\omega_2-\Omega,\omega_1)\times T^*(\omega_1,\Omega)T(\omega_2,\Omega)e^{-i(\omega_1-\omega_2)(\tau_T+\tau_0)}\right]. \tag{23}$$

For a system with the same constant conversion rate assumption and photon distribution as in Sec. II, we obtain

$$R_c(\tau_T)=\frac{T^2}{2}\left[1-e^{-(\Omega-\triangle)^2/(2\sigma_-^2)}e^{-\frac{1}{2}\sigma_-^2(\tau_T+\tau_0)^2}\right]. \tag{24}$$

The FWHM of $R_c(\tau_T)$ remains consistent with the simple $g^{(2)}$ function, as described in Eqs. (14) and (15). The position of the peak within the HOM dip yields insights into the delay, whereas the visibility, denoted as $e^{-(\Omega-\triangle)^2/(2\sigma_-^2)}$, within the dip provides information about the frequency shift Ω. As depicted in Fig. 4, the visibility of the HOM dip exhibits an increase when the frequency difference between the signal and idler photons decreases due to frequency conversion. It is worth noting that Eq. (24) highlights that the visibility of the HOM dip remains substantial as long as the parameter $f=\frac{\Omega-\triangle}{\sigma_-}\lesssim 1$. This condition aligns with reported experiments such as those in [18–20]. Consider a scenario where one utilizes an infrared (IR) photon alongside a visible photon to study HOM interference; under such circumstances, interference is scarcely observable. However, if the IR photon

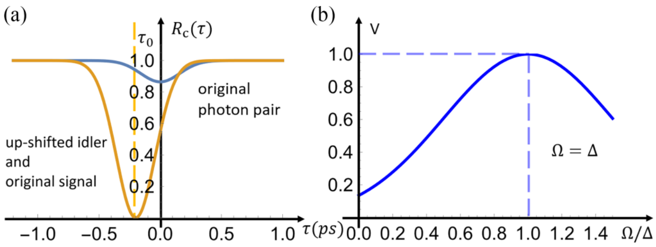

FIG. 4. (a) The $2R_c(\tau_T)/T^2$ function of the signal and up-converted idler photons (yellow), compared to the $R_c(\tau_T)$ of the original photon pair (blue), for $\sigma_- = 2\pi \times 1$ THz, $\tau_0 = 0.2$ ps, $\triangle = 2\pi \times 2$ THz and $\triangle - \Omega = 2\pi \times 0.05$ THz. (b) HOM dip visibility as a function of the shifted frequency Ω when $\sigma_- = 2\pi \times 1$ THz and $\triangle = 2\pi \times 2$ THz.

undergoes up-conversion into the visible part of the spectrum, robust HOM interference becomes evident. The HOM interference between photons of different colors was initially predicted by Raymer *et al.* [39] and subsequently experimentally validated by Kobayashi *et al.* [40]. In this context, two photons passing through an active beam-splitter undergo a conversion into each other's "color." For instance, the active beam-splitter transforms a red photon into a blue photon with a probability of 50% and vice versa. The situation in the research conducted by Tyumenev *et al.* [29] differs in that only the idler photon undergoes up-conversion. In this case, there is no mutual conversion between the signal and idler photons, and a passive beam-splitter, akin to the original HOM experiment, is employed. This distinction arises because the use of a passive beam-splitter necessitates that significant HOM interference occurs only when there is some overlap in the frequencies of the two photons. The interference becomes pronounced when the frequency difference, denoted as $(\Omega - \triangle)$, approaches zero. This explains why, in the study conducted by Kambs *et al.* [41], photons with wavelengths of 904 nm are converted into photons with wavelengths of 1557 nm, enabling the assessment of their indistinguishability.

Moving forward, we investigate the consequences of imperfect phase-matching within the up-conversion process using Eqs. (16) and (23). This analysis yields

$$R_c(\tau_T) = \frac{\sqrt{2}T^2\beta}{2}\left\{\frac{1}{\sqrt{4\sigma_p^2+\sigma_-^2+2\beta^2}}\exp\left(-\frac{2\Omega^2}{4\sigma_p^2+\sigma_-^2+2\beta^2}\right) - \frac{\beta}{\sqrt{(\beta^2+2\sigma_p^2)(2\beta^2+\sigma_-^2)}}\exp\left[-\frac{(\Omega+\triangle)^2}{4(\beta^2+2\sigma_p^2)}\right]\right.$$
$$\left.\times\exp\left[-\frac{(\Omega-\triangle)^2}{2\sigma_-^2} - \frac{\sigma_-^2\beta^2(\tau_T+\tau_0)^2}{2\beta^2+\sigma_-^2}\right]\right\}, \tag{25}$$

which reduces to Eq. (24) for $\beta^2 \to \infty$. Note that Eq. (25) shares the same FWHM as Eq. (19). From Eq. (25), we obtain the visibility of the HOM dip

$$V = \frac{\beta\sqrt{4\sigma_p^2+\sigma_-^2+2\beta^2}}{\sqrt{(\beta^2+2\sigma_p^2)(2\beta^2+\sigma_-^2)}}\exp\left[-\frac{(\Omega+\triangle)^2}{4(\beta^2+2\sigma_p^2)}\right]\exp\left[-\frac{(\Omega-\triangle)^2}{2\sigma_-^2}+\frac{2\Omega^2}{4\sigma_p^2+\sigma_-^2+2\beta^2}\right]. \tag{26}$$

The visibility is maximized when $\Omega = \triangle$ as

$$V = \frac{\beta\sqrt{4\sigma_p^2+\sigma_-^2+2\beta^2}}{\sqrt{\left(\beta^2+2\sigma_p^2\right)\left(2\beta^2+\sigma_-^2\right)}} \times\exp\left[-\frac{\left(8\sigma_p^2+\sigma_-^2+4\beta^2\right)\Omega^2}{\left(4\sigma_p^2+\sigma_-^2+2\beta^2\right)\left(\beta^2+2\sigma_p^2\right)}\right]. \tag{27}$$

When $\beta \gg \sigma_-$ and σ_p, the visibility approaches 1. However, an excellent visibility of 0.96 can still be achieved when $\beta \sim 2\sigma_-$ for a system, as depicted in Fig. 5(a). The FWHM depends both on σ_- and β. As shown in Fig. 5(b), when $\beta \sim 2\sigma_-$ the peak only undergoes a 50% expansion in comparison to the scenario where $\beta \gg \sigma_-$.

IV. CONCLUSION

Our theoretical investigation yields comprehensive insights into the influence of frequency conversion on the time-dependent quantum correlation of a photon pair. By deriving the second-order correlation function, we illustrate that the FWHM remains unaltered, while both the peak height and position undergo shifts following the up-conversion procedure. Remarkably, this observation aligns with recent experiments, as evidenced by the authors of Ref. [29], where the correlation time fell within the range of detector resolution time. This remains true when phase matching is satisfied across the spectral width of the idler photon.

In our quest to gain a deeper understanding of the ramifications of frequency up-conversion on quantum correlation, we delve into the intricacies of two-photon Hong-Ou-Mandel

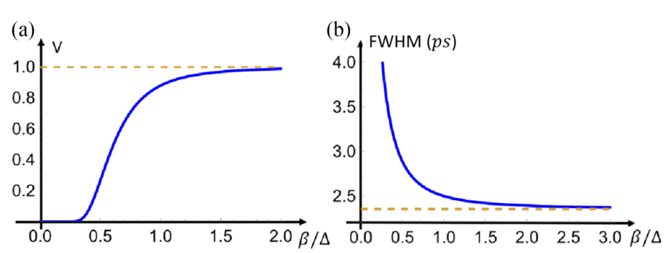

FIG. 5. (a) HOM dip visibility and (b) FWHM for both $R_c(\tau_T)$ and $g^2(\tau)$, as a function of the phase-matching factor β when $\sigma_- = 2\pi \times 1$ THz, $\sigma_p = \sigma_-/10$, $\triangle = 2\pi \times 2$ THz, and $\triangle - \Omega = 2\pi \times 0.05$ THz. The dashed lines indicate the limits when $\beta \gg \sigma_-$.

interferometry. Here, we demonstrate how the visibility of two-photon interference is sensitive to factors such as the magnitude of frequency change in the up-conversion process, the bandwidth of the signal photon, and the phase-matching factor β. It is noteworthy that these findings possess a level of generality and are anticipated to be applicable to various forms of frequency conversion.

ACKNOWLEDGMENTS

We thank the support of the Department of Energy (Grant No. FWP-ERW7011). G.S.A. and J.W. thank the Robert A. Welch Foundation (Grant No. A-1943) and A.V.S. thanks the Welch Foundation (Grant No. A-1547) for support.

[1] J. E. Midwinter and J. Warner, Up-conversion of near infrared to visible radiation in lithium-meta-niobate, J. Appl. Phys. **38**, 519 (1967).

[2] L. Ma, O. Slattery, and X. Tang, Single photon frequency up-conversion and its applications, Phys. Rep. **521**, 69 (2012).

[3] R. T. Thew, S. Tanzilli, L. Krainer, S. C. Zeller, A. Rochas, I. Rech, Sergio Cova, H. Zbinden, and N. Gisin, Low jitter up-conversion detectors for telecom wavelength GHz QKD, New J. Phys. **8**, 32 (2006).

[4] A. P. Vandevender and P. G. Kwiat, High efficiency single photon detection via frequency up-conversion, J. Mod. Opt. **51**, 1433 (2004).

[5] M. A. Albota and F. N. C. Wong, Efficient single-photon counting at 1.55 μm by means of frequency upconversion, Opt. Lett. **29**, 1449 (2004).

[6] C. Langrock, E. Diamanti, R. V. Roussev, Y. Yamamoto, M. M. Fejer, and H. Takesue, Highly efficient single-photon detection at communication wavelengths by use of upconversion in reverse-proton-exchanged periodically poled linbo 3 waveguides, Opt. Lett. **30**, 1725 (2005).

[7] L. Ma, O. Slattery, and X. Tang, Experimental study of high sensitivity infrared spectrometer with waveguide-based up-conversion detector, Opt. Express **17**, 14395 (2009).

[8] Y.-P. Huang, V. Velev, and P. Kumar, Quantum frequency conversion in nonlinear microcavities, Opt. Lett. **38**, 2119 (2013).

[9] S. Lefrancois, A. S. Clark, and B. J. Eggleton, Optimizing optical bragg scattering for single-photon frequency conversion, Phys. Rev. A **91**, 013837 (2015).

[10] A. Barh, P. J. Rodrigo, L. Meng, C. Pedersen, and P. Tidemand-Lichtenberg, Parametric upconversion imaging and its applications, Adv. Opt. Photonics **11**, 952 (2019).

[11] A. S. Ashik, C. F. O'Donnell, S. C. Kumar, M. Ebrahim-Zadeh, P. Tidemand-Lichtenberg, and C. Pedersen, Mid-infrared up-conversion imaging using femtosecond pulses, Photonics Res. **7**, 783 (2019).

[12] W. H. Louisell, A. Yariv, and A. E. Siegman, Quantum fluctuations and noise in parametric processes. I, Phys. Rev. **124**, 1646 (1961).

[13] J. Tucker and D. F. Walls, Quantum theory of parametric frequency conversion, Ann. Phys. (NY) **52**, 1 (1969).

[14] P. Kumar, Quantum frequency conversion, Opt. Lett. **15**, 1476 (1990).

[15] J. Huang and P. Kumar, Observation of quantum frequency conversion, Phys. Rev. Lett. **68**, 2153 (1992).

[16] H. J. McGuinness, M. G. Raymer, C. J. McKinstrie, and S. Radic, Quantum frequency translation of single-photon states in a photonic crystal fiber, Phys. Rev. Lett. **105**, 093604 (2010).

[17] S. Ates, I. Agha, A. Gulinatti, I. Rech, M. T. Rakher, A. Badolato, and K. Srinivasan, Two-photon interference using background-free quantum frequency conversion of single photons emitted by an inas quantum dot, Phys. Rev. Lett. **109**, 147405 (2012).

[18] L. Fan, C.-L. Zou, M. Poot, R. Cheng, X. Guo, X. Han, and H. X. Tang, Integrated optomechanical single-photon frequency shifter, Nat. Photonics **10**, 766 (2016).

[19] C. Chen, J. E. Heyes, J. H. Shapiro, and F. N. C. Wong, Single-photon frequency shifting with a quadrature phase-shift keying modulator, Sci. Rep. **11**, 300 (2021).

[20] D. Zhu, C. Chen, M. Yu, L. Shao, Y. Hu, C. J. Xin, M. Yeh, S. Ghosh, L. He, C. Reimer *et al.*, Spectral control of nonclassical light pulses using an integrated thin-film lithium niobate modulator, Light Sci. Appl. **11**, 327 (2022).

[21] C.-K. Hong, Z.-Y. Ou, and L. Mandel, Measurement of subpicosecond time intervals between two photons by interference, Phys. Rev. Lett. **59**, 2044 (1987).

[22] M. Barbieri, E. Roccia, L. Mancino, M. Sbroscia, I. Gianani, and F. Sciarrino, What Hong-Ou-Mandel interference says on two-photon frequency entanglement, Sci. Rep. **7**, 7247 (2017).

[23] S. P. Walborn, A. N. De Oliveira, S. Pádua, and C. H. Monken, Multimode Hong-Ou-Mandel interference, Phys. Rev. Lett. **90**, 143601 (2003).

[24] R.-B. Jin, R. Shiina, and R. Shimizu, Quantum manipulation of biphoton spectral distributions in a 2d frequency space toward arbitrary shaping of a biphoton wave packet, Opt. Express **26**, 21153 (2018).

[25] N. Fabre and S. Felicetti, Parameter estimation of time and frequency shifts with generalized Hong-Ou-Mandel interferometry, Phys. Rev. A **104**, 022208 (2021).

[26] T. Douce, A. Eckstein, S. P. Walborn, A. Z. Khoury, S. Ducci, A. Keller, T. Coudreau, and P. Milman, Direct measurement of the biphoton wigner function through two-photon interference, Sci. Rep. **3**, 3530 (2013).

[27] G. Boucher, T. Douce, D. Bresteau, Stephen P. Walborn, A. Keller, T. Coudreau, S. Ducci, and P. Milman, Toolbox for continuous-variable entanglement production and measurement using spontaneous parametric down-conversion, Phys. Rev. A **92**, 023804 (2015).

[28] X. Liu, T. Li, J. Wang, M. R. Kamble, A. M. Zheltikov, and G. S. Agarwal, Probing ultra-fast dephasing via entangled photon pairs, Opt. Express **30**, 47463 (2022).

[29] R. Tyumenev, J. Hammer, N. Y. Joly, P. S. J. Russell, and D. Novoa, Tunable and state-preserving frequency conversion of single photons in hydrogen, Science **376**, 621 (2022).

[30] A. V. Sokolov, Giving entangled photons new colors, Science **376**, 575 (2022).

[31] J. Hammer, M. V. Chekhova, D. R. Häupl, R. Pennetta, and N. Y. Joly, Broadly tunable photon-pair generation in a suspended-core fiber, Phys. Rev. Res. **2**, 012079(R) (2020).

[32] Y. Shih, *An Introduction to Quantum Optics: Photon and Biphoton Physics* (CRC Press, Boca Raton, FL, 2020).

[33] A. Eshun, B. Gu, O. Varnavski, S. Asban, K. E. Dorfman, S. Mukamel, and T. G. III, Investigations of molecular optical properties using quantum light and Hong–Ou–Mandel interferometry, J. Am. Chem. Soc. **143**, 9070 (2021).

[34] F. Bouchard, A. Sit, Y. Zhang, R. Fickler, Filippo M Miatto, Y. Yao, F. Sciarrino, and E. Karimi, Two-photon interference: the Hong–Ou–Mandel effect, Rep. Prog. Phys. **84**, 012402 (2021).

[35] A. Hochrainer, M. Lahiri, M. Erhard, M. Krenn, and A. Zeilinger, Quantum indistinguishability by path identity and with undetected photons, Rev. Mod. Phys. **94**, 025007 (2022).

[36] A. Lyons, G. C. Knee, E. Bolduc, T. Roger, J. Leach, E. M. Gauger, and D. Faccio, Attosecond-resolution Hong-Ou-Mandel interferometry, Sci. Adv. **4**, eaap9416 (2018).

[37] G. Di Martino, Y. Sonnefraud, M. S. Tame, S. Kéna-Cohen, F. Dieleman, Ş. K. Özdemir, M. S. Kim, and S. A. Maier, Observation of quantum interference in the plasmonic Hong-Ou-Mandel effect, Phys. Rev. Appl. **1**, 034004 (2014).

[38] B. Ndagano, H. Defienne, D. Branford, Y. D. Shah, A. Lyons, N. Westerberg, E. M. Gauger, and D. Faccio, Quantum microscopy based on Hong–Ou–Mandel interference, Nat. Photonics **16**, 384 (2022).

[39] M. G. Raymer, S. J. van Enk, C. J. McKinstrie, and H. J. McGuinness, Interference of two photons of different color, Opt. Commun. **283**, 747 (2010).

[40] T. Kobayashi, R. Ikuta, S. Yasui, S. Miki, T. Yamashita, H. Terai, T. Yamamoto, M. Koashi, and N. Imoto, Frequency-domain Hong–Ou–Mandel interference, Nat. Photonics **10**, 441 (2016).

[41] B. Kambs, Quantum frequency conversion of indistinguishable photons from independent solid state emitters, Ph.D. thesis, Saarland University Thesis, 2019.